

# Dynamics of Cockroach Ocellar Neurons

MAKOTO MIZUNAMI, HIDEKI TATEDA, and KEN-ICHI NAKA

From the Department of Biology, Kyushu University, Fukuoka 812, and the National Institute for Basic Biology, Okazaki 444, Japan

**ABSTRACT** The incremental responses from the second-order neurons of the ocellus of the cockroach, *Periplaneta americana*, have been measured. The stimulus was a white-noise-modulated light with various mean illuminances. The kernels, obtained by cross-correlating the white-noise input against the resulting response, provided a measure of incremental sensitivity as well as of response dynamics. We found that (a) the incremental sensitivity of the second-order neurons was an exact Weber-Fechner function; (b) white-noise-evoked responses from second-order neurons were linear; (c) the dynamics of second-order neurons remain unchanged over a mean illuminance range of 4 log units; (d) the small nonlinearity in the response of the second-order neuron was a simple amplitude compression; and (e) the correlation between the white-noise input and spike discharges of the second-order neurons produced a first-order kernel similar to that of the cell's slow potential. We conclude that signal processing in the cockroach ocellus is simple but different from that in other visual systems, including vertebrate retinas and insect compound eyes, in which the system's dynamics depend on the mean illuminance.

## INTRODUCTION

Insects have two kinds of visual organs, the compound eye and the ocellus. The former has been the subject of extensive study; the latter has received less attention. There is evidence that the ocellus plays an important role in the insect's visual behavior (Goodman, 1981; Taylor, 1981*a, b*). The insect ocellar retina contains many (>100) photoreceptors and a small number of (<12) large second-order neurons, called L-cells (Goodman, 1981). Recordings from insect ocellar neurons were first made extracellularly by Ruck (1957, 1961) and intracellularly by Chappell and Dowling (1972). These authors showed that light stimulation depolarized the ocellar receptors and hyperpolarized the L-cells. Subsequent studies in locusts (Patterson and Goodman, 1974; Wilson, 1978; Simmons, 1982*a*), dragonflies (Chappell and DeVoe, 1975; Patterson and Chappell, 1980; Simmons, 1982*b*), bees (Milde, 1981, 1984), and cockroaches (Mizunami et al., 1982) have confirmed Chappell and Dowling's original observation that ocellar L-cells produce hyperpolarization, but have also shown that the patterns of the light-evoked responses are different in different insects.

Address reprint requests to Dr. M. Mizunami, Dept. of Biology, Faculty of Science, 33, Fukuoka 812, Japan.

In the past, most of the functional studies on ocellar neurons have been performed with steps of light given in the dark, as in most of the studies on other visual systems. Consequently, not much is known about the cell's response dynamics or how they respond to modulation around a mean illuminance, which is the condition in which ocellar neurons function in the natural environment. One notable exception is the study of Chappell and Dowling (1972), who measured incremental responses of dragonfly ocellar L-cells and concluded that the incremental threshold of their offset responses is a Weber-Fechner function over a 5-log range of mean illuminance.

In this study, we stimulated the cockroach ocellus with white-noise-modulated light, and analyzed response dynamics of ocellar neurons by cross-correlating the light inputs with the resulting cellular responses. The methodology, referred to as white-noise analysis, enabled us to define incremental sensitivity as well as response dynamics over a large range of mean illuminance. We analyzed the responses of the second-order neurons, L-cells, recorded intracellularly. We found that (a) the modulation responses were linear and the first-order kernels could predict cellular responses with mean square errors (MSEs) of  $\sim 10\%$ ; (b) the incremental sensitivity was an exact Weber-Fechner function over a 4-log range of mean illuminance; (c) waveforms of kernels remained unchanged over the same mean illuminance range: the response dynamics were independent of mean illuminance; (d) the small second-order nonlinearity was accounted for by a simple compression of the hyperpolarizing first-order kernel: no complex nonlinearity was found in the L-cell response; and (e) correlation of spike discharges with the white-noise inputs produced first-order kernels very similar to those from slow potentials.

## MATERIALS AND METHODS

### *Biological*

Adult male cockroaches, *Periplaneta americana*, reared in the laboratory of Kyushu University, were used. The cockroach was rigidly mounted on a Lucite stage and its head was immobilized using beeswax. The compound eyes and the other ocellus were light-shielded with beeswax mixed with carbon black. The cockroach survived several days under this condition. For recording from second-order neurons, the cuticle between the two ocelli was removed and the ocellar nerve was exposed. The exposed tissue was treated with 1% pronase type IV (Sigma Chemical Co., St. Louis, MO) in cockroach saline (Yamasaki and Narahashi, 1959) for 1 min, to facilitate electrode penetration. Recordings were made with a glass pipette filled either with potassium acetate (2 M) or potassium citrate (2 M). Both electrodes (resistances of 50–80 M $\Omega$ ) produced similar results. The indifferent electrode (a platinum wire) was placed in a saline pool in which the exposed tissues were bathed.

Fig. 1 shows a schematic representation of the system for measuring the light (input) and response (output). The light source was either a glow tube (R-1130B, Sylvania/GTE, Exeter, NH) or a light-emitting diode (Sharp Corp., Tokyo, Japan). The spectral composition of the glow tube was nearly flat from 400 to 700 nm, whereas that of the light-emitting diode had a peak at 560 nm. Both stimuli produced similar results. A series of neutral-density (ND) filters attenuated the light beam in 1-log steps. The white-noise signal was obtained from a random signal generator (WG-772, NF Circuit Design Block,

Tokyo, Japan). The depth of modulation defined in a conventional fashion,  $(I_{\max} - I_{\min}) / (I_{\max} + I_{\min})$ , was  $\sim 0.7-0.9$  at 0 dB. The depth of modulation of the white-noise signal is an approximation because of the statistical nature of the input. Light signals were monitored by a photodiode (TFA1001W, Siemens-Allis, Inc., Cherry Hill, NJ) before they were attenuated by filters. Light stimulus and cellular responses were initially stored on analog tape and analyzed offline on a VAX 11/780 computer (Digital Equipment Corp., Maynard, MA) with an API20B array processor (Floating Point Systems, Portland, OR).

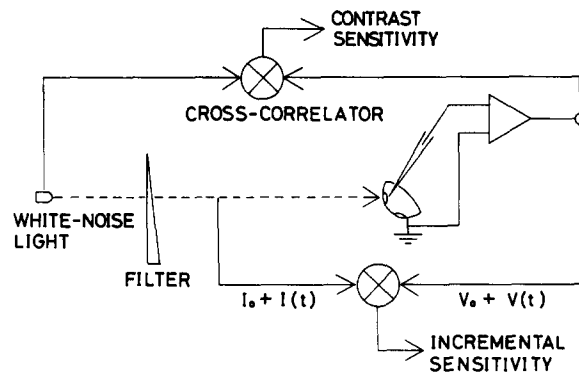


FIGURE 1. Schematic drawing of experimental procedure. The light source was either a glow modulator or a light-emitting diode. A series of ND filters were interposed between the light source and the preparation to attenuate both the mean illuminance and white-noise modulation by the same proportion, so that the “contrast” of the stimulus was kept unchanged. The light signal was monitored before it was attenuated by filters and a correlation was made between the unattenuated light signal and the cellular response. The correlation produced kernels on a contrast sensitivity scale. Kernels were converted to an incremental sensitivity scale by multiplying the kernel’s amplitude by the attenuation factor.

### *Analytical*

The light stimulus the cockroach received daily or nightly consisted of two parts, one with a steady mean,  $I_0$ , and the other with a modulation around the mean,  $I(t)$ , as shown in Fig. 4. The mean illuminance,  $I_0$ , changes slowly but covers a large range. The modulation depth of fluctuation around the mean illuminance, however, is moderate and should remain roughly constant. The response evoked therefore consists of two components, the steady mean,  $V_0$ , and the modulation response,  $V(t)$ , the former being related to  $I_0$  and the latter to  $I(t)$ . The peak of the step-evoked response,  $V_p$ , may be different from  $V_0$ . The relationship between  $I_0$  and  $V_p$  or  $V_0$  is a cell’s DC (static) sensitivity: how a cell responds to steps of light given in the dark. The classic example is Naka-Rushton relationship (Naka and Rushton, 1966). The relationship between  $I(t)$  and  $V(t)$  has been obtained by measuring the threshold, i.e., the intensity of stimulus that produces a just-detectable response, the classic example being the Weber-Fechner relationship. However, the responses of visual neurons that do not produce spike discharges have no threshold that can easily be defined. In a white-noise analysis, the relationship between  $I(t)$  and  $V(t)$  is represented by kernels obtained by cross-correlating the white-noise input with the resulting cellular response. The results of first-order cross-correlation, weighted by the power of the stimulus, are

the first-order kernels. The first-order kernel is the linear part of the cell's response to an impulse input superposed on a mean illuminance. If a cell's response is linear or quasilinear, the amplitude and waveform of first-order kernels are therefore the comprehensive measure of a cell's incremental sensitivity and the response dynamics. If a cell's response contains second-order nonlinear components, the first- and second-order kernels represent the linear and nonlinear components of the cell's incremental response, and their amplitudes and waveforms represent the cell's incremental sensitivity and response dynamics (Sakuranaga and Ando, 1985).

The spikes evoked by white-noise stimulus can also be analyzed as in the case of the analog response. A correlation was made between the spike discharges (a point process), which were transformed into 5-ms pulses, and a white-noise input. The resulting kernels are interpreted as the post-synaptic potential, which triggers a spike discharge (Ando, Y.-I., M. Sakuranaga, and K.-I. Naka, manuscript in preparation).

In actual experiments, the light signal was monitored before it was attenuated by ND filters, and a correlation was made between the monitored light signal,  $10^n \cdot I(t)$ , and the modulation response,  $V(t)$ , where  $n$  is the log attenuation factor of the filters. The DC components in both signals,  $I_0$  and  $V_0$ , were subtracted out before correlation. The results of the correlation were kernels whose amplitude was on a contrast sensitivity scale. The kernel's ordinate values could be converted to an incremental sensitivity scale by multiplying their amplitude scale by the attenuation factor,  $10^n$ , i.e., for a 1-log filter by 10, for a 2-log filter by 100, etc. Conversion is only for the amplitude and does not affect the waveform of kernels.

The linearity of a cell's response can be assessed if we know how well the linear model obtained by convolving the original white-noise signal with the first-order kernel matches the recorded cellular response. The degree of accuracy is the MSE. The theoretical aspects of the analysis are described by Sakuranaga and Ando (1985), and algorithms for computing first- and second-order kernels, model responses, and MSEs can be found in Chappell et al. (1985).

## RESULTS

The cockroach has two ocelli, one at the base of each antenna (Fig. 2A). Each ocellar retina contains ~10,000 photoreceptors, and they converge on four large second-order neurons, or L-cells (Weber and Renner, 1976). As shown in Fig. 2B, the L-cell has extensive dendritic branches in the ocellus (Mizunami et al., 1982), where the neuron receives what appear to be ribbon synapses from the photoreceptor axons (Weber and Renner, 1976; Toh and Sagara, 1984). The axon of the L-cell projects into the brain through the ocellar nerve. In the brain, L-cells make synaptic contacts with third-order neurons (Toh and Hara, 1984; Mizunami et al., 1986). In this study, intracellular recordings from L-cells were made from the axonal region of the ocellar nerve. Stable recordings could be made for 30–60 min.

Fig. 3A shows the responses of an L-cell evoked by 250-ms flashes whose illuminance was increased in 1-log steps. The responses to brief steps of light showed sustained hyperpolarization, and a few (one to four) spikes were seen on the depolarizing phase of the offset response. Note that the sustained nature of the response was due to the short duration of the stimulus (cf. Fig. 4): with continued stimulation, the membrane potential depolarized to a new steady level,  $V_0$ . Fig. 3B shows the  $V$ -log  $I$  plot, in which the peak response amplitudes,  $V_p$ , is plotted against the log of stimulus illuminance,  $I_0$ . The curve, an average from

five L-cells, is S-shaped, which relates to the cell's static (DC) sensitivity. A similar S-shaped function was seen in L-neurons of locusts (Wilson, 1978), bees (Milde and Homberg, 1984), and dragonflies (Chappell and DeVoe, 1975).

Fig. 4 shows the L-cell's responses evoked by steps and white-noise-modulated stimuli. Brief steps of light given in the dark produced step-like responses with a peak,  $V_p$ . A spike is seen at the offset of the stimulus. The relationship between the amplitude of the step stimulus,  $I_o$ , and the peak of resulting response,  $V_p$ , is

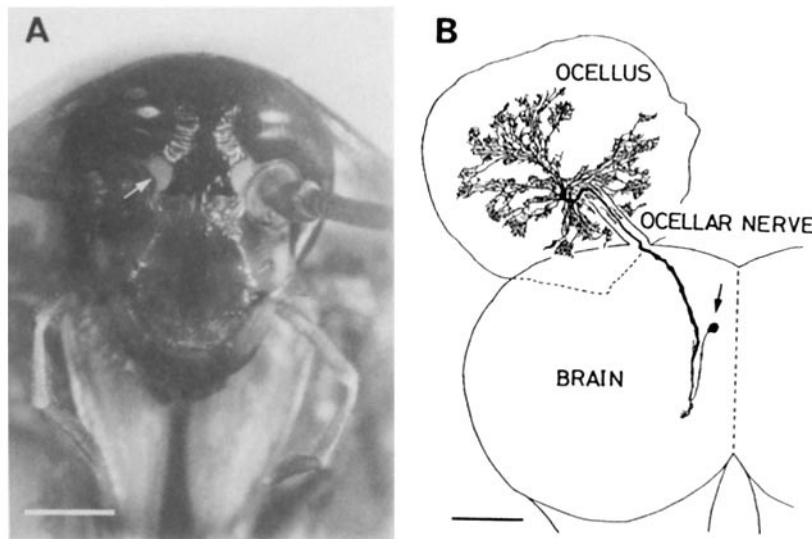


FIGURE 2. (A) Head of a cockroach. The cockroach has a pair of ocelli (arrow) at the base of the antenna, in addition to the compound eyes. (B) Ocellar second-order neuron (L-cell) viewed dorsally. The drawing is from a cobalt-filled neuron. L-cells extend their dendritic branches into the ocellar retina, and receive inputs from a large number of photoreceptors. The axon of the L-cell projects into the ocellar tract of the brain, through the ocellar nerve. In the ocellar tract, the L-neurons make output synapses onto a number of the third-order neurons (Toh and Hara, 1984). The cell body is located in the brain (arrow). Scale: 1 mm (A); 200  $\mu\text{m}$  (B).

shown in Fig. 3. At the beginning of white-noise stimulation, a transient peak similar to the one produced by steps of light was seen. With continued white-noise stimulation, the membrane potential reached a steady level,  $V_o$ , within 30–40 s. The steady level was maintained as long as the stimulus was continued, i.e., the L-cell reached a dynamic steady state. At the steady state, the depolarizing phase of the slow potential fluctuation often exceeded the membrane potential observed in the dark. This is clearly seen in the probability distribution function (PDF) of the response in Fig. 5C. The kernels were computed by cross-correlating the slow potentials or spike discharges against the white-noise inputs during the dynamic steady state. Spike potentials were removed with a low-pass filter (0.1–50 Hz) for slow potential analysis. For analysis of spike discharge, a trigger circuit produced standard pulses of 5 ms for each spike discharge.

Fig. 5A shows the slow responses of an L-cell produced by white-noise stimuli with modulation depths of 0, -10, and -20 dB but with the same mean illuminance of  $20 \mu\text{W}/\text{cm}^2$ . The response produced by stimuli with various modulation depths had the same steady mean hyperpolarization, but the amplitude of the modulation response changed in proportion to the modulation depth of the stimulus. To clarify this observation, first-order kernels were computed from a longer (80–100 s) record for each depth of modulation. The three kernels from 0, -10, and -20 dB stimuli had identical amplitudes and waveforms (Fig.

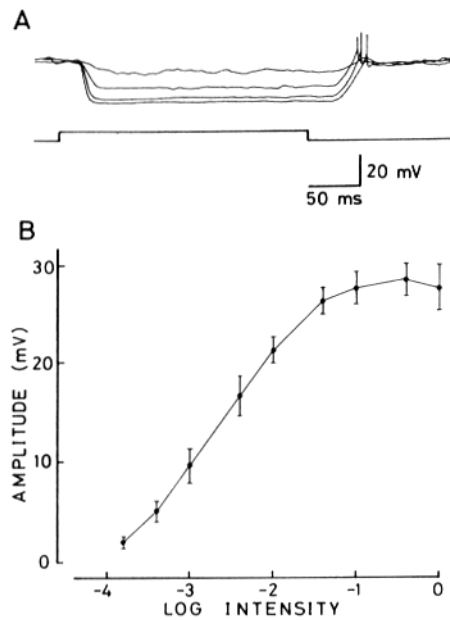


FIGURE 3. Step-evoked responses from an L-cell. Four responses evoked by light stimuli with 0, 1, 2, and 3 log attenuating filters are shown. The illuminance of stimulus without filters (0 log) was  $30 \mu\text{W}/\text{cm}^2$ . A few spikes are seen at the offset of the stimuli. (B) Relationship between the amplitude of step-evoked response and the magnitude of step stimulus. An average from five L-cells is shown with the standard deviations.

5B). The incremental sensitivity and response dynamics, which are the amplitudes and waveforms of the kernels, did not depend on the modulation depth of the stimulus, which is what we would expect from a linear system. Fig. 5C shows three pairs of PDFs from 0, -10, and -20 dB records, each pair being the PDF for the light stimulus and response. The PDFs are plotted on an absolute scale, in millivolts for the response and in microwatts per square centimeter for the light stimulus. First the PDFs were computed from a section of a record after the removal of the DC components as described in Materials and Methods. The levels of mean hyperpolarization,  $V_o$ , were measured from the original record (one example is shown in Fig. 4) and the PDFs were plotted so that they represented the modulation around the mean hyperpolarization,  $V_o$ . The PDFs

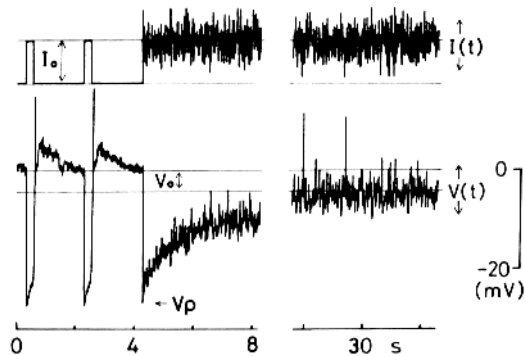


FIGURE 4. Responses from an L-cell evoked either by steps of light given in the dark or by white-noise-modulated light. The relationship between  $I_o$  and  $V_p$  or  $V_o$  is the cell's DC (static) sensitivity and the relationship between  $I(t)$  and  $V(t)$  is the incremental sensitivity. Spike potentials are seen at the offset of step stimulation as well as during white-noise stimulation.

for the response and stimulus of the three pairs matched well. PDFs of white-noise stimuli are Gaussian, and, if a system is linear, the PDF of its response to a Gaussian white-noise stimulus must be Gaussian. The observations shown in Fig. 5 indicate that (a) the mean level of hyperpolarization was produced by the mean illuminance,  $I_o$ : as long as the mean illuminance remains unchanged, the mean hyperpolarization remains unchanged; (b) the cell's modulation response was

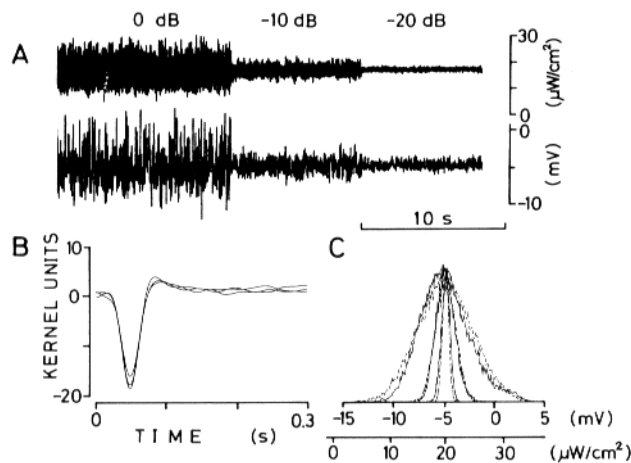


FIGURE 5. Responses evoked by a white-noise stimulus of 0, -10, and -20 dB in the depth of modulation. (A) Time records in which upper trace is for light and lower trace is for response. 0 mV in the amplitude scale indicates the membrane potential in the dark. Note that the mean hyperpolarization remained unchanged. (B) First-order kernels for the three segments of the white-noise record. The noisy kernel was for the -20 dB record. The kernel's units are millivolts per microwatt per square centimeter per second. (C) Three pairs of PDFs for the three white-noise segments. Each pair consists of response and light stimulus PDFs.

linear because the three kernels produced by white-noise stimulus of three depths of modulation were identical; and (c) the linearity of the modulation response is also suggested by the PDFs.

If the response of a cell is linearly related to the stimulus modulation, the cell's response to the modulation should be predictable from the first-order kernels with a fair degree of accuracy. Fig. 6A shows the time records of the white-noise stimulus (upper trace) and the resulting response (lower traces in a continuous

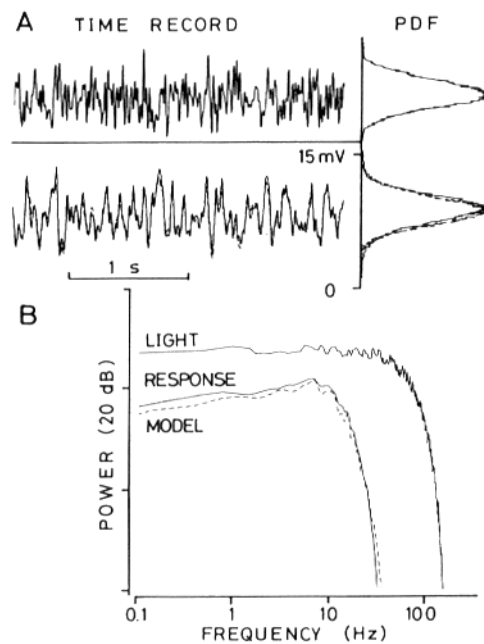


FIGURE 6. Time records of part of a white-noise stimulus and the resulting cellular response (continuous line). Superposed on the response trace is the linear model (broken line). PDFs for the light stimulus and the recorded response are also shown. The light PDF is also superposed on the response PDF. In *B*, power spectra of the light stimulus, response (continuous line), and model (broken line) are shown. The mean illuminance of the stimulus is  $20 \mu\text{W}/\text{cm}^2$ .

line). Superposed on the response trace is the model response predicted by the first-order kernel (broken line). Although there are occasional deviations, the two traces matched well, which shows that the response could be predicted from the first-order kernel fairly accurately. Indeed, the averaged MSE computed from five L-cells was 11.1%, with a standard deviation of 2.1%. Fig. 6A also shows the PDFs of the light stimulus and of the response PDF. The light stimulus PDF is also superimposed on the response. Although there is a minor deviation between the two PDFs near the mean, they were in good agreement. Fig. 6B shows the power spectra of the light stimulus, response, and model. The power spectrum of the response (continuous line) matched well that of the model shown by the broken line. Both had a peak at  $\sim 8$  Hz and had a slight bandpass-filtering



property, as seen by the lower power for the low-frequency region. A similar analysis made on the responses at a mean illuminance level of  $20\text{--}0.002 \mu\text{W}/\text{cm}^2$  showed that the responses produced by white-noise modulation were linear. The response produced by a stimulus with a mean illuminance of  $<0.002 \mu\text{W}/\text{cm}^2$  had a much larger MSE ( $>30\%$ ), probably because of the noise in the response. We allowed the animal to adapt to the low illuminance stimulus light for  $\sim 15$  min, but the MSE of the response was still  $>30\%$ .

If a system is linear, the system's response to any arbitrary stimulus should be predictable from its first-order kernels. Fig. 7 shows an example in which the L-cell's response was evoked by a stimulus modulated by a sinusoidal sweep. In the figure, the prediction (model) obtained by convolving the stimulus with the first-

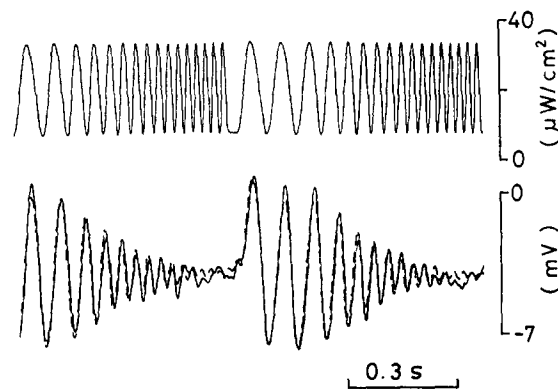


FIGURE 7. Response of an L-cell to a stimulus modulated by a sinusoidal sweep (10–40 Hz). The light stimulus (upper trace), response (lower trace, solid line), and linear model (dashed line) are shown.

order kernels (broken line) is superposed on the actual response (solid line). The two traces match well, as expected from a linear system. The observations in Figs. 5–7 indicate that the modulation response from the cockroach L-cell is almost linear and therefore the first-order kernels are good approximations of the cell's incremental sensitivity and response dynamics.

Fig. 8A shows the kernels obtained at five mean illuminance levels, plotted on a contrast sensitivity scale. In this experiment, a cell was impaled and the retina was dark-adapted for 5 min; the test began with a 5-log ND filter interposed. After each white-noise test run, which started after 90 s of adaptation to the stimulus light and lasted for 90 s, the density of the ND filter was decreased in 1-log steps. After the test by the maximum illuminance (0 log), the sequence was reversed. Both sequences produced similar results. The kernels were hyperpolarizing and monophasic (integrating). The waveforms were identical, with constant peak response times of  $\sim 50$  ms, and the amplitudes differed by only 30%. This is remarkable because the mean illuminance for which the kernels were computed covered a range of 1:10,000. Stimuli dimmer than  $-4$  log units produced no reliable results, although we allowed the animal to adapt to the

stimuli for 15 min. For comparison, kernels from a horizontal cell of the turtle, *Pseudemys scripta elegans*, obtained under comparable conditions, are shown in Fig. 8B. Note that the turtle's cellular response could be predicted from the first-order kernels with MSEs of <10% (Chappell et al., 1985). In the turtle's horizontal cell, the amplitude of the kernels on a contrast sensitivity scale decreased as the mean illuminance decreased. As the mean illuminance was

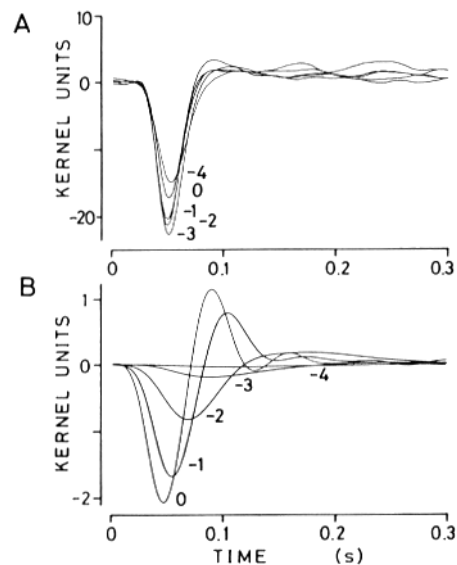


FIGURE 8. (A) First-order kernels, plotted on a contrast sensitivity scale, obtained at five mean levels. The first-order kernels were calculated by cross-correlating the white-noise light stimuli with the recorded responses. Kernels are labeled 0 through  $-4$  to indicate the log density of the filters interposed. Note that the amplitudes of the kernels did not differ by more than 30% and the peak response times were constant at 50 ms for all kernels, although the mean levels covered a range of 1:10,000. Stimuli dimmer than  $-4$  log units did not produce any reliable results. B shows turtle horizontal cell kernels plotted as in A. The peak response times, waveforms, and amplitudes differed for different levels of mean illuminance. Kernel units are in millivolts per microwatt per square centimeter per second. The larger incremental sensitivity for ocellar kernels was due to the dimmer mean illuminance ( $20 \mu\text{W}/\text{cm}^2$  at 0 log) of the white-noise stimulus than in the turtle experiment ( $50 \mu\text{W}/\text{cm}^2$  at 0 log).

increased, the peak response times became shorter from 100 to 50 ms and the waveform became more biphasic (differential). Thus, the response dynamics depend on the mean illuminance. Sets of impulse responses or kernels similar to the one shown in Fig. 8B have been obtained in the human visual system (Kelly, 1971) and lower vertebrate horizontal cells (Naka et al., 1979; Chappell et al., 1985).

Fig. 9A shows the relationship between the amplitudes of the kernels on an incremental sensitivity scale and the level of mean illuminance. The plots, averaged from five L-cells, are on a straight line with a slope of  $-1$ : this is the

Weber-Fechner relationship, which shows that for a 10-fold increase in the mean illuminance, the incremental sensitivity decreases by a factor of 10 (i.e., the contrast sensitivity is independent of the mean illuminance). Fig. 9B shows the peak response times of kernels used to produce plots in Fig. 9A. For a 4-log range of mean illuminance, the peak response times remained virtually unchanged at 50 ms. This shows that the mean illuminance controlled only the scaling of incremental sensitivity, but not the response dynamics.

Although the L-cell's response to white-noise-modulated light was linear, there was a small degree of nonlinearity. The second-order kernel represents

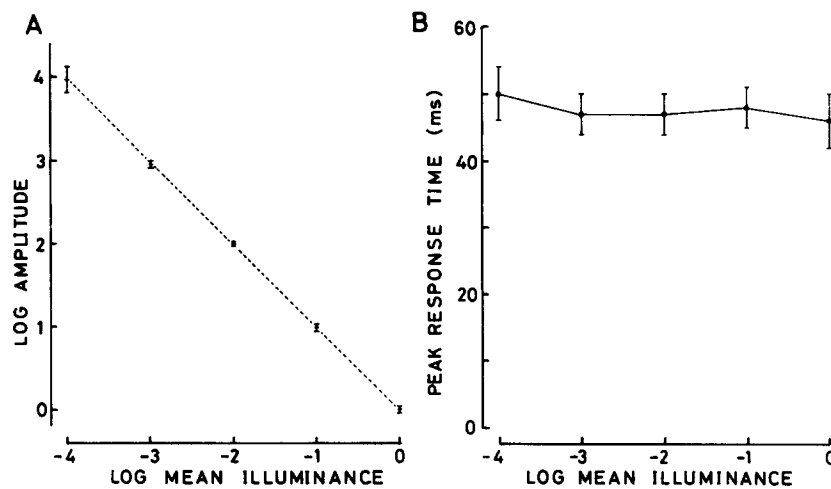


FIGURE 9. Incremental sensitivity plotted against mean illuminance. The ordinate is the amplitude of the first-order kernels on an incremental sensitivity scale, and was  $25 \text{ mV}/(\mu\text{W}/\text{cm}^2) \cdot \text{s}$  at 0 log. The plot is an exact Weber-Fechner relationship. The peak response times of kernels at five mean illuminance levels are plotted in B. The peak response times were almost constant at  $\sim 50$  ms over the 4-log range of mean illuminance. In A and B, averages from five L-cells are shown with standard deviations.

the nonlinearity produced by an interaction of two pulses. The second-order kernel is therefore a three-dimensional solid with two time axes,  $\tau_1$  and  $\tau_2$ , which represent the time relationships of two pulses. Fig. 10A shows an example of a second-order kernel from the L-cell's response. The second-order kernel had a (depolarizing) peak on the diagonal, which indicates that the nonlinearity is produced when two pulses are given concurrently. The second-order kernel shows that the magnitude of responses increases somewhat nonlinearly with the increase in the stimulus magnitude, because two stimuli given concurrently are equivalent to twice the increase in the stimulus amplitude. Fig. 10B shows the diagonal cut (side view) of the second-order kernel together with the first-order kernel. The waveforms of the kernels are mirror images of each other, which indicates that (a) hyperpolarization by the first-order kernel is opposed by depolarization caused by the second-order kernel: the nonlinearity was for a simple amplitude compression; (b) the nonlinearity was involved in the generation

of the L-cell's slow response, because the waveform (time course) of the second-order kernel was almost the same as that of the first-order kernel. A similar nonlinearity has been observed in vertebrate horizontal cells (Naka et al., 1979; Chappell et al., 1985).

The second-order kernel had no off-diagonal peak, which indicates that there is no nonlinear interaction of two pulses coming at any time interval. That is,

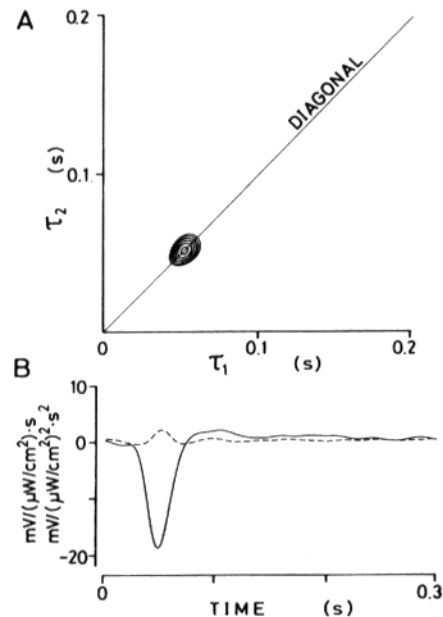


FIGURE 10. Typical second-order kernel from L-cells. (A) Contour map of a second-order kernel with two axes,  $\tau_1$  and  $\tau_2$ . The magnitude of the second-order kernel is shown by the contour lines. The kernel is a solitary depolarizing peak on the diagonal, which indicates that the nonlinear response is depolarizing and is produced when two pulses of lights are given simultaneously. The nonlinearity is therefore produced by an increase in the stimulus amplitude. (B) First-order kernel (solid line) and the diagonal cut (side view) of the second-order kernel (broken line) shown in A. The waveforms are mirror images of each other, which shows that the nonlinearity was of the simple compression type. As the second-order nonlinearity is a quadratic function, the amplitude of the second-order kernel is a quadratic function of the input magnitude, whereas the amplitude of the first-order kernel is linearly related to the input amplitude. The ordinate units in B are for the first-order kernel only.

the responses produced by two pulses coming at an interval of  $t$  ( $t = \tau_1 - \tau_2$ ) are identical, and the two identical responses produced by two flashes sum linearly. In a system in which the summation is not linear and the response produced by the second pulse is affected by the first pulse, a deviation from linearity appears on the off-diagonal region, where  $\tau_1 \neq \tau_2$ . One such example is shown in Fig. 11, in which an intracellular recording was made from a catfish (*Ictalurus punctatus*) ganglion cell. A decremental flash produced transient on-off depolar-

izations from the cell (Fig. 11A). Although the cell's response included both the slow and spike components, our unpublished results show that the correlation of the white-noise input with either the spike or slow component produced a similar second-order kernel. The second-order kernel of the cell's slow potential shown in Fig. 11B is much more complex than the one from a cockroach L-cell (Fig. 10A) and is composed of two on-diagonal depolarizing peaks and two off-diagonal

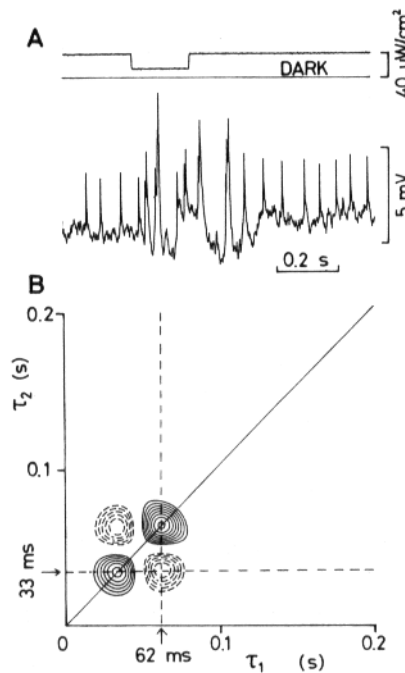


FIGURE 11. A response from a catfish ganglion cell produced by a decremental flash from a steady illuminance of  $40 \mu\text{W}/\text{cm}^2$  (A) and a second-order kernel of the cell's slow potentials (B). In B, the continuous contour lines are peaks and the broken contour lines are valleys in the second-order kernels. A second-order kernel represents the nonlinearity related to the timing of two pulses. Nonlinear interactions of two pulses arriving at the same time ( $\tau_1 = \tau_2$ ) produced two on-diagonal depolarizing peaks, whereas two successive pulses arriving with a delay of 29 ms produced off-diagonal hyperpolarizing valleys. The latter point is illustrated in the figure by measuring the peak time of one of the valleys indicated by the intersection of two broken lines, which are 62 ms for  $\tau_1$  and 33 ms for  $\tau_2$ , i.e.,  $62 - 33 = 29$  ms.

hyperpolarizing valleys. The second-order kernel is similar to those from type-C amacrine cells in catfish retina and is responsible for producing on-off transient depolarizations evoked by step inputs (Sakuranaga and Naka, 1985). In the cockroach L-cell, the amplitude of the response is simply related to the instantaneous amplitude of the input stimulus, whereas in the catfish ganglion cell, the response is generated by more complex signal-processing.

The L-cells of the cockroach produced spikes at the offset of the step input, as did those of bees (Milde, 1981) and locusts (Wilson, 1978). An example of the

spikes produced by a white-noise stimulus is shown in Fig. 4. To discover the relationship between the stimulus and the spike discharge, we cross-correlated the spike discharge with the white-noise stimulus. As shown in Fig. 12A, the normalized first-order kernel of spike discharge is hyperpolarizing, as is the kernel of the slow potential (computed from the slow potential in the same record), and their waveforms are very similar. We detected a latency of  $\sim 5$ – $8$  ms between the two kernels. The fixed latency of the spike kernels suggests that the site of spike generation is some distance from the site of slow potential generation. The second-order kernel of spike discharge was a solitary depolarizing peak on the diagonal (Fig. 12B), and the waveforms of its diagonal cut was

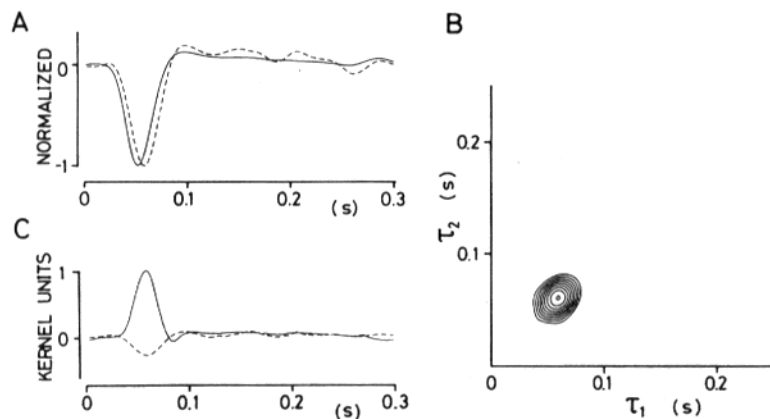


FIGURE 12. Typical first- and second-order kernels of spike discharge of L-cells. (A) First-order kernel of spike discharge (broken line) and slow potentials from the same record (solid line). The kernels are normalized for comparison of their waveforms. (B) Typical second-order kernel. The kernel is a solitary depolarizing peak on the diagonal. (C) First-order kernel (broken line) and the diagonal cut of the second-order kernel (solid line). The waveforms are mirror images of each other.

a mirror image of the first-order kernel (Fig. 12C). The results suggest that no complex nonlinearity is involved in the spike generation. For a step decrement from a mean illuminance, we can predict a depolarization (excitation) from the spike first-order kernel. The depolarization is augmented by a depolarization from the second-order kernel, and will trigger spike discharge. The generation of spikes is related to the instantaneous amplitude of the input stimulus, but not to any particular timing hidden in the stimulus.

#### DISCUSSION

The first intracellular recordings from insect ocellus were made by Chappell and Dowling (1972), who showed that a light stimulus depolarized the ocellar receptors and hyperpolarized the second-order neurons. They also showed that the incremental threshold of the offset depolarizing responses of the second-order neurons is a Weber-Fechner function. Although many reports on the insect ocellus have followed (Goodman, 1981), the responses in these studies were

evoked by flashes of light given in the dark and measurements were made on the static aspects of the step-evoked responses.

We used white-noise-modulated light to evoke responses from cockroach ocellar neurons. Cockroaches in their natural environment do not experience a flashing spot of light in the dark. Their photic inputs fluctuate around a mean illuminance, and their visual systems including ocelli must be developed to appreciate changes around a mean illuminance, not a sudden flash in darkness. In our earlier studies on the horizontal cells in the retinas of the turtle (Chappell et al., 1985), catfish (Naka et al., 1979), and skate (manuscript submitted for publication), the response dynamics of (hyperpolarizing) second-order neurons were examined with white-noise stimuli that mimic the inputs the retina receives in its natural environment. We found for the cockroach L-cell that (a) the incremental responses were linear with MSEs of  $\sim 10\%$ , (b) the cell's incremental sensitivity was an exact Weber-Fechner function over a mean illuminance range of 4 log units, and (c) the response dynamics remain unchanged in the same range of mean illuminance. These observations indicate that the levels of mean illuminance controlled the amplitude scaling of the incremental response but not its dynamics. This is a remarkable finding because the response dynamics, as well as the incremental sensitivity of all the visual systems so far studied, depend upon the levels of mean illuminance. This is the case with *Limulus* photoreceptors (Fuortes and Hodgkin, 1964), photoreceptors of insects compound eyes (Pinter, 1972; Dubs, 1981), vertebrate cones (Baylor and Hodgkin, 1973) and second-order neurons (Naka et al., 1979; Tranchina et al., 1983, 1984; Chappell et al., 1985), and the human visual system (Kelly, 1971). Such a coupling has been one of the principal features of models of visual systems (Fuortes and Hodgkin, 1964; Kelly, 1971). This study shows that the couplings of sensitivity and dynamics are not necessarily ubiquitous characteristics of the visual system.

We could not measure incremental responses at a mean illuminance of  $< 0.002 \mu\text{W}/\text{cm}^2$ , because the responses were much smaller than the noise at that low illuminance. With a very long exposure to a very low-illuminance light, the sensitivity might be improved and the incremental responses might be measured. The dynamics of incremental responses at a very low mean illuminance may be different from those observed in the present experiment, if indeed they exist.

The response of ocellar L-cells to a steady or modulated stimulus is characterized by the loss of the steady hyperpolarizing component,  $V_o$ , i.e.,  $V_o$  is much smaller than  $V_p$ . This response characteristic appears as a large initial transient hyperpolarization, but the ratio of  $V_p$  to  $V_o$  differs among the L-cells of several insects. In the dragonfly (Klingham and Chappell, 1978) and bee (Milde, 1981, 1984; Milde and Homberg, 1984), the steady state response of L-cells has almost no steady component,  $V_o$ . In the cockroach, as shown here, and possibly in the locust (Wilson, 1978), the response of L-cells retains a small steady hyperpolarization. The transient nature of the L-cell's response indicates that L-cells respond mainly to changes in mean illuminance,  $I(t)$ , but not to the mean magnitude,  $I_o$ . The transient nature of the response yields the characteristic incremental sensitivity function. A similar analysis of the response dynamics of the ocelli of other insects should produce results very similar to those found in the cockroach ocellus.

Spike discharges seen in the L-cell have been associated with the offset of the step stimulus (Ruck, 1957; Mizunami et al., 1982). In some insects, the ocellar L-cells produced spontaneous discharges that were suppressed by steady illumination (dragonflies: Chappell and Dowling, 1972; bees: Milde, 1981, 1984). In this study, we found that (a) the first-order kernel for spike discharge was hyperpolarizing; (b) the second-order nonlinearity was a simple, on-diagonal depolarization; and (c) the waveform (dynamics) of the first-order kernel for spike discharge was identical to that of the slow potential kernel. These findings suggest that the slow potential, when depolarized to a sufficient degree, produced spike discharges: there was no complex signal transformation between the generation of the slow potential and that of spike discharges. As the first-order kernel is hyperpolarizing for both slow and spike responses, a depolarization (excitation) is produced by a decremental stimulus. The function of spikes of L-cells is to detect dimming from a mean illuminance.

In conclusion, we propose a sandwich model for the cockroach ocellus. Receptors and (slow potentials of) L-cells form a linear filter whose gain, but not dynamics, is controlled by the mean illuminance in such a fashion that for a 10-fold increase in the mean illuminance, the gain decreases by exactly 1/10. This is a piecewise linearization. The production of a spike discharge in L-cells is a nonlinear process, and the correlation between the white-noise input and the spike discharges identifies the linear and lower-order nonlinear filters. The lower-order, probably a second-order, nonlinearity produces a depolarization (excitation), which, together with the (linear) depolarization produced by a dimming from a mean illuminance, produces a spike discharge. The linear filter for a spike discharge corresponds to the preceding linear filter formed by the slow responses of L-cells.

The horizontal cells in the vertebrate retina are second-order neurons that receive inputs from a large number of receptors. In vertebrates, both the receptors and the (majority of) horizontal cells produce a hyperpolarizing response. In the ocellus, the receptors depolarize and the second-order cells, which also receive inputs from a large number of receptors, hyperpolarize. In the vertebrate retina, transmission is sign-noninverting, whereas in the ocellus it is sign-inverting. Although the sign of signal transmission is opposite, the L-cell and vertebrate horizontal cells share many features: (a) the response to a white-noise stimulus is almost linear; (b) the incremental sensitivity is Weber-Fechner-like, although in the horizontal cell, sensitivity is approximately a Weber-Fechner function, but in the L-cell, it is exactly a Weber-Fechner function; and (c) the small nonlinearity was for amplitude compression: no complex nonlinearity was found. As we have already discussed, the crucial difference was that the dynamics of the incremental response from all vertebrate horizontal cells were dependent upon the levels of mean illuminance, whereas in cockroach ocellus the response dynamics was independent of the level of illumination.

We thank Yu-Ichiro Ando, National Institute for Basic Biology, Okazaki, Japan, for his assistance in analysis and Dr. Masanori Sakuranaga, Canon Research Center, Canon Corp., Atsuki, Japan, for his suggestions. The results shown in Fig. 11 were provided by Dr. Hiroko M. Sakai, National Institute for Basic Biology.

*Original version received 21 February 1986 and accepted version received 23 May 1986.*



## REFERENCES

- Baylor, D. A., and A. L. Hodgkin. 1973. Detection and resolution of visual stimuli by turtle photoreceptors. *Journal of Physiology*. 234:163–198.
- Chappell, R. L., and R. D. DeVoe. 1975. Action spectra and chromatic mechanisms of cells in the median ocelli of dragonflies. *Journal of General Physiology*. 65:399–419.
- Chappell, R. L., and J. E. Dowling. 1972. Neural organization of the median ocellus of the dragonfly. I. Intracellular electrical activity. *Journal of General Physiology*. 60:121–147.
- Chappell, R. L., K.-I. Naka, and M. Sakuranaga. 1985. Dynamics of turtle horizontal cell response. *Journal of General Physiology*. 86:423–453.
- Dubs, A. 1981. Non-linearity and light adaptation in the fly photoreceptors. *Journal of Comparative Physiology*. 144:53–59.
- Fuortes, M. G. F., and A. L. Hodgkin. 1964. Changes in time scale and sensitivity in the ommatidia of *Limulus*. *Journal of Physiology*. 172:239–263.
- Goodman, L. J. 1981. Organization and physiology of the insect dorsal ocellar system. In *Handbook of Sensory Physiology*. Vol. VII/6C. Springer-Verlag, Berlin. 201–286.
- Kelly, D. H. 1971. Theory of flicker and transient responses. I. Uniform fields. *Journal of the Optical Society of America*. 61:537–546.
- Klingham, A., and R. L. Chappell. 1978. Feedback synaptic interaction in the dragonfly ocellar retina. *Journal of General Physiology*. 71:157–175.
- Milde, J. J. 1981. Graded potentials and action potentials in the large ocellar interneurons of the bee. *Journal of Comparative Physiology*. 143:427–434.
- Milde, J. J. 1984. Ocellar interneurons in the honey bee: structure and signals of L-neurons. *Journal of Comparative Physiology*. 154:683–693.
- Milde, J. J., and U. Homberg. 1984. Ocellar interneurons in the honey bee: characteristics of spiking L-neurons. *Journal of Comparative Physiology*. 155:151–160.
- Mizunami, M., and H. Tateda. 1986. Classification of ocellar interneurons in the cockroach brain. *Journal of Experimental Biology*. In press.
- Mizunami, M., S. Yamashita, and H. Tateda. 1982. Intracellular stainings of the large ocellar second order neurons in the cockroach. *Journal of Comparative Physiology*. 149:215–219.
- Naka, K.-I., R. Y. Chan, and S. Yasui. 1979. Adaptation in catfish retina. *Journal of Neurophysiology*. 42:441–454.
- Naka, K.-I., and W. A. H. Rushton. 1966. S-potentials from luminosity units in the retina of fish (Cyprinidae). *Journal of Physiology*. 185:587–599.
- Patterson, J. A., and R. L. Chappell. 1980. Intracellular responses of procion filled cells and whole nerve cobalt impregnation in the dragonfly median ocellus. *Journal of Comparative Physiology*. 139:25–39.
- Patterson, J. A., and L. J. Goodman. 1974. Intracellular responses of receptor cells and second-order cells in the ocelli of the desert locust, *Schistocerca gregaria*. *Journal of Comparative Physiology*. 95:237–250.
- Pinter, R. B. 1972. Frequency and time domain properties of reticular cells of the desert locust (*Schistocerca gregaria*) and the house cricket (*Acheta domesticus*). *Journal of Comparative Physiology*. 77:383–397.
- Ruck, P. 1957. The electrical responses of dorsal ocelli in cockroaches and grasshoppers. *Journal of Insect Physiology*. 1:109–123.
- Ruck, P. 1961. Electrophysiology of the insect dorsal ocellus. I. Origin of components of the electroretinogram. *Journal of General Physiology*. 44:605–627.
- Sakuranaga, M., and Y.-I. Ando. 1985. Visual sensitivity and Wiener kernels. *Vision Research*. 25:507–510.

- Sakuranaga, M., and K.-I. Naka. 1985. Signal transmission in the catfish retina. III. Transmission to type C-cell. *Journal of Neurophysiology*. 53:411-428.
- Simmons, P. J. 1982a. Transmission mediated with and without spikes at connexions between large second-order neurons of locust ocelli. *Journal of Comparative Physiology*. 147:401-414.
- Simmons, P. J. 1982b. The operation of connexions between photoreceptors and large second-order neurons in dragonfly ocelli. *Journal of Comparative Physiology*. 149:389-398.
- Taylor, C. P. 1981a. Contribution of compound eyes and ocelli to steering of locusts in flight. I. Behavioural analysis. *Journal of Experimental Biology*. 93:1-18.
- Taylor, C. P. 1981b. Contribution of compound eyes and ocelli to steering of locusts in flight. II. Timing changes in flight motor units. *Journal of Experimental Biology*. 93:19-31.
- Toh, Y., and S. Hara. 1984. Dorsal ocellus system of the American cockroach. II. Structure of the ocellar tract. *Journal of Ultrastructure Research*. 86:135-148.
- Toh, Y., and H. Sagara. 1984. Dorsal ocellar system of the American cockroach. I. Structure of the ocellus and ocellar nerve. *Journal of Ultrastructure Research*. 86:119-134.
- Tranchina, D., J. Gordon, and R. Shapley. 1983. Spatial and temporal properties of luminosity horizontal cells in the turtle retina. *Journal of General Physiology*. 82:573-598.
- Tranchina, D., J. Gordon, and R. Shapley. 1984. Retinal adaptation—evidence for a feedback mechanism. *Nature*. 310:314-316.
- Weber, G., and M. Renner. 1976. The ocellus of the cockroach, *Periplaneta americana* (Blattariae). Receptory area. *Cell and Tissue Research*. 168:209-222.
- Wilson, M. 1978. The functional organization of locust ocelli. *Journal of Comparative Physiology*. 124:297-316.
- Yamasaki, T., and T. Narahashi. 1959. The effects of potassium and sodium ions on the resting and action potentials of the cockroach giant axon. *Journal of Insect Physiology*. 3:146-158.